horticulturae

MDPI

Article

Characterization and Isolation of Piperamides from *Piper nigrum* Cultivated in Costa Rica

Luis Felipe Vargas-Huertas [1], Luis Diego Alvarado-Corella [1], Andrés Sánchez-Kopper [2], Andrea Mariela Araya-Sibaja [3] and Mirtha Navarro-Hoyos [1,*]

[1] Bioactivity for Sustainable Development (BIODESS), Department of Chemistry, University of Costa Rica (UCR), Rodrigo Facio Campus, San Pedro Montes Oca, San José 2060, Costa Rica; luis.vargashuertas@ucr.ac.cr (L.F.V.-H.); luis.alvaradocorella@ucr.ac.cr (L.D.A.-C.)
[2] Department of Chemistry, Technological University of Costa Rica (TEC), Cartago 7050, Costa Rica; ansanchez@itcr.ac.cr
[3] Laboratorio Nacional de Nanotecnología LANOTEC-CeNAT-CONARE, Pavas, San José 1174, Costa Rica; aaraya@cenat.ac.cr
* Correspondence: mnavarro@codeti.org; Tel.: +506-8873-5539

Abstract: The piperamides profile of *Piper nigrum* cultivated in Costa Rica was studied using ultra-performance liquid chromatography coupled with electrospray ionization quadrupole time-of-flight high-resolution mass spectrometry (UPLC-ESI-QTOF-HRMS) on enriched-piperamides extracts. A total of 31 different piperamides were identified, 24 of them with a methylenedioxyphenyl moiety, including piperine and nine other compounds with the characteristic piperidine ring, as well as guineensine, retrofractamide B, and eight other piperamides with an *N*-isobutyl group. In addition, piperyline and two other compounds with a pyrrolidine ring, as well as piperflaviflorine B, holding a *N*-2-methylbutyl chain, were characterized. In turn, pellitorine and six other piperamides exhibiting a long olefinic chain instead of the methylenedioxyphenyl group were also tentatively identified. In addition, quantification was performed using UPLC coupled with a diode array detector (UPLC-DAD), with 15 piperamides being quantified, including piperine, piperyline, piperanine, and piperloguminine with values within the range of previous reports, while results obtained for guineensine (276.5–421.0 mg/100 g dry material) and pellitorine (414.4–725.0 mg/100 g dry material) were higher than those reported in the literature. Additionally, preparative and semi-preparative high-performance liquid chromatography (HPLC) separations allowed to isolate, besides piperine, four other piperamides, which were identified through HRMS, ^{1}H and ^{13}C nuclear magnetic resonance (NMR). These included retrofractamide B, guineensine, pellitorine, and (2*E*,4*E*,12*Z*)-*N*-isobutyl-octadeca-2,4,12-trienamide, with yields of 134.0 mg/100 g dry material, 209.7 mg/100 g dry material, 361.8 mg/100 g dry material and 467.0 mg/100 g dry material, respectively, with all these values higher than those reported in previous studies in the literature. The findings constitute the first report of such a number and diversity of compounds in *P. nigrum* cultivated in Costa Rica.

Keywords: *Piper nigrum*; black pepper; UPLC ESI-MS; piperamides; piperine; guineensine; pellitorine; retrofractamide B

Citation: Vargas-Huertas, L.F.; Alvarado-Corella, L.D.; Sánchez-Kopper, A.; Araya-Sibaja, A.M.; Navarro-Hoyos, M. Characterization and Isolation of Piperamides from *Piper nigrum* Cultivated in Costa Rica. *Horticulturae* **2023**, *9*, 1323. https://doi.org/10.3390/horticulturae9121323

Academic Editors: Jelena Popović-Djordjević, Luiz Fernando Cappa de Oliveira, Haroon Khan and Sina Siavash Moghaddam

Received: 8 November 2023
Revised: 27 November 2023
Accepted: 28 November 2023
Published: 9 December 2023

1. Introduction

Black pepper (*Piper nigrum*) is a fruit cultivated worldwide because of its commercial interest, holding a high position in total production among the main fruit crops used as spices worldwide [1]. The International Trade Center (ITC) in Geneva, Switzerland, estimates the current trade in spices at 400,000–450,000 metric tons with a total value of US USD 1.5–2 billion annually. With an annual growth rate of 3.6% in quantity and 8.4% in value in spices, pepper contributes 34% of total trade in spices [2].

With a practice spanning thousands of years, ayurvedic practitioners have long prescribed black pepper, as it was a key component in many ayurvedic remedies in India and

likely enhanced the effectiveness of other compounds in traditional herbal medicines [3]. Likewise, its positive influence on the bioavailability of drugs and nutrients has been reported, increasing intestinal absorption and regulating metabolism and transport [4]. Recent reports have described that piperine enhances the solubility of natural metabolites and drugs through the formation of multicomponent organic materials (MOMs), for instance, forming eutectic mixtures with drugs and naturally occurring compounds and boosting their solubility, dissolution rate, and wettability while decreasing contact angle [5].

Reviews on the use of *P. nigrum* highlighted the in vivo neuroprotective and hypoglycemic effects presenting a potential for further research, especially to investigate its capacity to inhibit acetylcholinesterase and butyrylcholinesterase, two enzymes critically implicated in Alzheimer's and Parkinson's disorders, but also α-amylase, α-glucosidase, and lipase enzymes [6] as well as other neuroprotective properties reducing caffeine-induced effects on mice hyperlocomotion [7].

In turn, extracts derived from *Piper nigrum* have exhibited notable antibacterial efficacy against a spectrum of microorganisms, including *Candida albicans*, *Escherichia coli*, various *Aspergillus* species, diverse *Bacillus* strains, various *Pseudomonas* variants, several *Staphylococcus* strains, and *Salmonella* species, showing its broad antibacterial effects [8]. It was also observed that *P. nigrum* extracts restored the antioxidant profile and normalized levels of urea and creatinine and the renal histological architecture after the induction of renal toxicity in rats via monosodic glutamate [9]. In addition, immunomodulatory functions related to the modulation of cellular energy metabolism have been reported [10].

Piperine, the most abundant amide in *P. nigrum*, exerts anti-inflammatory, neuroprotective, immunomodulatory, cardioprotective, and anticancer effects [11], for instance, including inhibition of growth and differentiation of cancer cells through various pathways, including ROS (reactive oxygen species) generation, caspase-mediated apoptosis, the inhibition of cell migration, the suppression of oncogene expression, and the enhancement of mitochondrial-mediated pathways [12].

Other amides from *Piper* spp. have gained interest because of their bioactive properties, such as inhibitors of cellular uptake of the endocannabinoid anandamide. Structure–activity studies emphasize the significance of the alkyl chain length in molecules like guineensine, which inhibits endocannabinoid uptake across various cell lines independently of fatty acid hydrolase (FAAH) [13] and exhibits significant neuro-pharmacological interactions with sigma receptors, 5-hydroxy-tryptamine 2A (5-HT2A) receptors, dopamine transporters (DATs), and 5-hydroxy-tryptamine 2B (5-HT2B) receptors when tested against 45 central nervous system (CNS)-related receptors, channels, and transporters [14].

Piperine also inhibits enzymes like cytochrome P450 3A4 (CYP3A4), which in turn affect drug interactions. For instance, it impacts how the organism processes such drugs as nevirapine, carbamazepine, midazolam, diclofenac sodium, and glimepiride because of CYP enzyme inhibition [15]. With these drugs, botanical interaction is important to highlight since such properties can pose a challenge in terms of public safety concerns, and therefore, quality assessment on the characterization and quantification of metabolites on raw materials and final goods based on *P. nigrum* is of particular interest.

In turn, pellitorine inhibits lipid accumulation during adipogenesis in 3T3 Swiss albino cell line (3T3-L1) cells and protects vascular barrier integrity by reducing hyperpermeability, cell adhesion molecule (CAM) expression, and leukocyte adhesion and migration [16,17]. Meanwhile, retrofractamide B, along with guinensine and *N*-isobutyl di and trienamides, has shown analgesic gastroprotective effects in experimental ethanol- and indomethacin-induced gastric lesions in rats [18].

Based on these important reports of pharmacological effects and potential applications, interest in developing or incorporating black pepper extracts or piperamides in final products in the dietary supplements and drug industry is expected to continue to grow, and the secondary metabolic profile can be used as a tool to provide relevant markers for predicting future pharmacological applications. Hence, the aim of this study was the characterization of piperamides of commercial black pepper cultivated in Costa Rica via

UPLC-ESI-QTOF-HRMS, as well as their quantification using UPLC-DAD and further isolation of different piperamides of interest because of their bioactive properties.

2. Materials and Methods

2.1. Plant Material

P. nigrum commercialized fruits were acquired in a dry state from one of the main local Costa Rican distributors, corresponding to different producers from the northern part of the country, and harvested in the peak season. Namely, samples Pn-d and Pn-f pertained to the San Carlos region, and Pn-j pertained to the Guatuso region. Furthermore, Pn-d, Pn-j, and Pn-f were harvested in the months of December, January, and February, respectively. These regions have different altitudes, corresponding to 40 masl (meters above sea level) for Guatuso and 266 masl for San Carlos, as well as different temperatures and rainfall. Considering the harvest month for each sample, the annual average temperature was 27.2 °C for Pni-j and 25.8 °C for Pn-d and Pn-f, while the annual average rainfall was 411.6, 182.5, and 395 mm for Pn-d, Pn-j, and Pn-f, respectively. The samples were kept in sealed containers at −20 °C.

2.2. Reagents and Solvents

Reagents such as piperine (97%) and formic acid (99%) were provided by Sigma-Aldrich (St. Louis, MO, USA). Solvents of ACS (American Chemical Society, Washington, DC, USA) and HPLC grade, such as acetonitrile (99.8%), ethyl acetate (99.7%), ethyl ether (99%), methanol (99.8%), and water (100%), were purchased from Baker (Center Valley, PA, USA), while deuterated chloroform (99.8%) and deuterated methanol (98.8%) were acquired from Sigma-Aldrich (St. Louis, MO, USA). Calibration and lock spray kits from Waters (Milford, MA, USA) were used to prepare sodium formate and leucine enkephalin solutions.

2.3. Piperamide Extracts from P. nigrum Fruits

P. nigrum dry fruits were extracted in a Dionex™ ASE™ 150 Accelerated Solvent Extractor (Thermo Scientific™, Walthman, MA, USA) using ethyl acetate as a solvent in a 34 mL cell at room temperature. The extract was washed with water, and then, the organic solvent was eliminated under vacuum to obtain a piperamides-rich extract.

2.4. UPLC-QTOF-ESI MS Analysis

Measurements were performed using a Xevo G2-XS QTOF (Waters, UK) coupled with an AQUITY H Class UPLC system with a quaternary pump. ESI source parameters were set to a capillary voltage of 2 kV, sampling cone of 20 eV, source temperature of 150 °C, source offset of 10 °C, desolvation temperature of 450 °C, cone gas flow of 0 L/h, and desolvation gas flow of 900 L/h. The measurement was performed in MS^e high-resolution positive mode using an acquisition mass range from 100 m/z to 1000 m/z and a scan rate of 0.5 s. Instrument calibration was performed in the mass range of the measurement with sodium formate. Lock mass correction was applied directly to the measurement using leucine enkephalin infusion measured each 30 s during the run. The data were analyzed using MassLynx V4.2 software from Waters. A 1 µL sample was injected with a flow of 0.5 mL/min using a Luna C18 column (150 mm × 4.6 mm id × 4 µm; Phenomenex, Torrance, CA, USA) at 30 °C and a chromatographic gradient starting at 40% B increasing to 100% B at 30 min; the gradient was held for 7 min, and then, the column was equilibrated for 5 min to initial conditions. Solvents used in the mobile phase were A water with 0.1% formic acid and B acetonitrile with 0.1% formic acid.

2.5. UPLC-DAD Quantification of Piperamides

For quantification purposes, measurements were performed using a method previously reported in the literature [19] with some modifications for optimization. Briefly, a calibration curve of piperine was performed between 10 and 1000 mg/L using a UPLC-

DAD coupled with a simple quadrupole MSQ instrument (ThermoFisher Scientific, San Jose, CA, USA) and a Synergi Polar RP column (150 mm × 4.6 mm id × 4 µm; Phenomenex, Torrance, CA, USA). Mobile phases A and B consisted of a combination of 0.1% formic acid in water (*v*/*v*) and 0.1% formic acid in acetonitrile (*v*/*v*), respectively. The linear gradient was from 40% to 70% B (*v*/*v*) at 17 min to 100% B at 24 min and held at 100% B to 27 min. The PDA acquisition was set at 260 nm and 340 nm. *P. nigrum* extract samples were measured under the same conditions. Results are expressed as mg of piperine equivalents and as a percentage of each piperamide in the extract composition, calculated by considering the integrated area for each peak as a percentage of the sum of all areas.

2.6. Preparative and Semipreparative HPLC for Piperamides Isolation

A total of 10 mL of cold ethyl ether was added to the pepper extract, stirred to dissolve completely, concentrated in a rotary evaporator at 20 °C to half the volume, and left to rest in a cold bath for 15 min. The remaining solid was separated via vacuum filtration and allowed to air dry. The solid obtained constituted piperine (PIP), while the filtrate (SBN) was used for subsequent purifications.

The SBN extract was dissolved at 1 g/mL in methanol, and 200 µL were injected using a preparative column (Phenomenex Luna C12(2) 250 × 21.2 mm, 5 µm) with elution at 7.0 mL/min using water (A), methanol (B) and acetonitrile (C). The gradient started with 55% B and 35% C and was maintained for 8 min, then increased to 50% B and 25% C at 10 min, maintained constant until 13 min, and then increased to 60% B and 40% C at 18 min and remained constant until 30 min. Fractions were collected and evaporated to dryness and then analyzed via UPLC-MS and NMR

Fraction 4 was subjected to a subsequent semipreparative process with a Synergi Polar-RP column (150 × 10 mm id, 4 µm; Phenomenex, Torrance, CA) using water (A) and acetonitrile (B) with a gradient from 50% B to 62.4% B in 7 min, 70% B at 13 min and up to 80% B at 20 min with a flow rate of 3.8 mL/min. Fractions were collected and evaporated to dryness and then analyzed via UPLC-MS and NMR.

2.7. Nuclear Magnetic Resonance Analysis

Analyses were performed with 5 mg of each compound dissolved in 0.75 mL of deuterated chloroform or deuterated methanol. Measurements were performed in a Bruker Ascend 400 MHz instrument, and chemical shifts (δ) are reported in ppm relative to internal tetramethylsilane (TMS, δ = 0.0 ppm) as standard.

2.8. Statistical Analysis

One-way analysis of variance (ANOVA), followed by Tukey's post hoc test, was applied to piperamides quantification values, and differences were considered significant at $p < 0.05$.

3. Results and Discussion

3.1. Profile by UPLC-QTOF-ESI MS Analysis of Piperamides

The UPLC-QTOF-ESI MS analysis could identify 31 piperamides in the extracts from *P. nigrum* commercial dry fruits, prepared as described in the Materials and Methods section, from the three different commercial dry samples, namely Pn-d, Pn-j, and Pn-f. Extracts were obtained as oleoresins with an average yield of 8.62%. Table 1 and Figure 1 summarize the results of the piperamides identification analysis.

Table 1. Profile of piperamides identified by UPLC-QTOF-ESI-MS analysis for *P. nigrum* samples.

Peak	Tentative Identification	Rt (min)	$[M + H]^+$ (Da)	Molecular Formula	Error (ppm)	MS^2 Fragments
1	Piperlonguminine	11.17	274.1420	$C_{16}H_{20}NO_3$	−8.46	201, 173,135
2	Piperylline	11.33	272.1327	$C_{16}H_{18}NO_3$	4.81	201, 171, 143, 135
3	Dihydropiperlonguminine	13.26	276.1586	$C_{16}H_{22}NO_3$	−4.96	173, 145, 135
4	Piperanine	14.12	288.1602	$C_{17}H_{22}NO_3$	0.80	203, 175, 145, 161, 135
5	Piperine	14.32	286.1273	$C_{17}H_{20}NO_3$	−9.48	201, 171, 143, 135
6	Piperdardine	17.22	314.1794	$C_{19}H_{24}NO_3$	2.04	199, 161
7	(2*E*,4*E*,8*E*)-Piperamide-C9:3	17.53	326.1804	$C_{20}H_{24}NO_3$	4.66	227, 197
8	Piperettine	18.44	312.1655	$C_{19}H_{22}NO_3$	17.72	227, 199, 169
9	Retrofractamide A	18.90	328.1944	$C_{20}H_{26}NO_3$	9.54	255, 227, 161, 135
10	Pipercallosine	20.07	330.2108	$C_{20}H_{28}NO_3$	1.75	229, 135
11	Pellitorina	20.17	224.2015	$C_{14}H_{26}NO$	0.27	208, 168, 154
12	Dehydropipernonaline	20.65	340.1971	$C_{21}H_{26}NO_3$	7.14	255, 227, 179, 161, 135
13	Pipernonaline	21.90	342.2122	$C_{21}H_{28}NO_3$	5.43	229, 227, 199, 161, 135
14	Retrofractamide B	22.86	356.2261	$C_{22}H_{30}NO_3$	9.91	283, 255, 161, 135
15	Piperolein B	23.45	344.2272	$C_{21}H_{30}NO_3$	3.45	201, 135
16	Piperchabamide D	24.13	358.2411	$C_{22}H_{32}NO_3$	8.04	285, 227, 135
17	Piperundecalidine	24.97	368.2231	$C_{23}H_{30}NO_3$	1.44	255, 135
18	Piperchabamide B	26.39	370.2446	$C_{22}H_{32}NO_3$	8.72	285, 161, 135
19	Brachiamide A	26.54	382.2458	$C_{24}H_{32}NO_3$	9.83	311, 283, 161, 135
20	Guineensine	26.95	384.2591	$C_{24}H_{34}NO_3$	3.61	311, 283, 161, 135
21	Piperflaviflorin A	27.99	386.2699	$C_{24}H_{36}NO_3$	0.99	313, 135
22	Piperflaviflorin B	28.35	398.2727	$C_{25}H_{36}NO_3$	7.99	283, 161, 135
23	Piperchabamide C	29.09	396.2575	$C_{25}H_{34}NO_3$	9.16	311,283, 161, 135
24	Brachistamide B	30.49	412.2857	$C_{26}H_{38}NO_3$	1.29	339, 311, 161, 135
25	1-(octadeca-2*E*,4*E*,12/13*Z*-trienoyl)pyrrolidine	32.14	332.2957	$C_{22}H_{38}NO$	1.08	304, 261, 233
26	Brachistamide D	34.75	426.3001	$C_{27}H_{40}NO_3$	−1.69	135
27	(2*E*,4*E*,13*Z*)-*N*-isobutyl-2,4,13-octadecatrienamide	35.18	334.3147	$C_{22}H_{40}NO$	1.10	306, 261
28	1-(octadeca-2*E*,4*E*,12/13*Z*-trienoyl)pyrrolidine	36.20	332.2957	$C_{22}H_{38}NO$	1.08	304, 261, 233
29	(2*E*,4*E*)-*N*-isobutyl-2,4-octadecadienamide	36.76	336.3070	$C_{22}H_{42}NO$	−8.40	320, 280, 263
30	1-(octadeca-2*E*,4*E*,13*Z*-trienoyl)piperidine	38.56	346.3136	$C_{23}H_{40}NO$	7.54	318, 261
31	(2*E*,4*E*,14*Z*)-*N*-Isobutyl-2,4,14-eicosatrienamide	39.92	362.3423	$C_{24}H_{44}NO$	0.03	306, 289

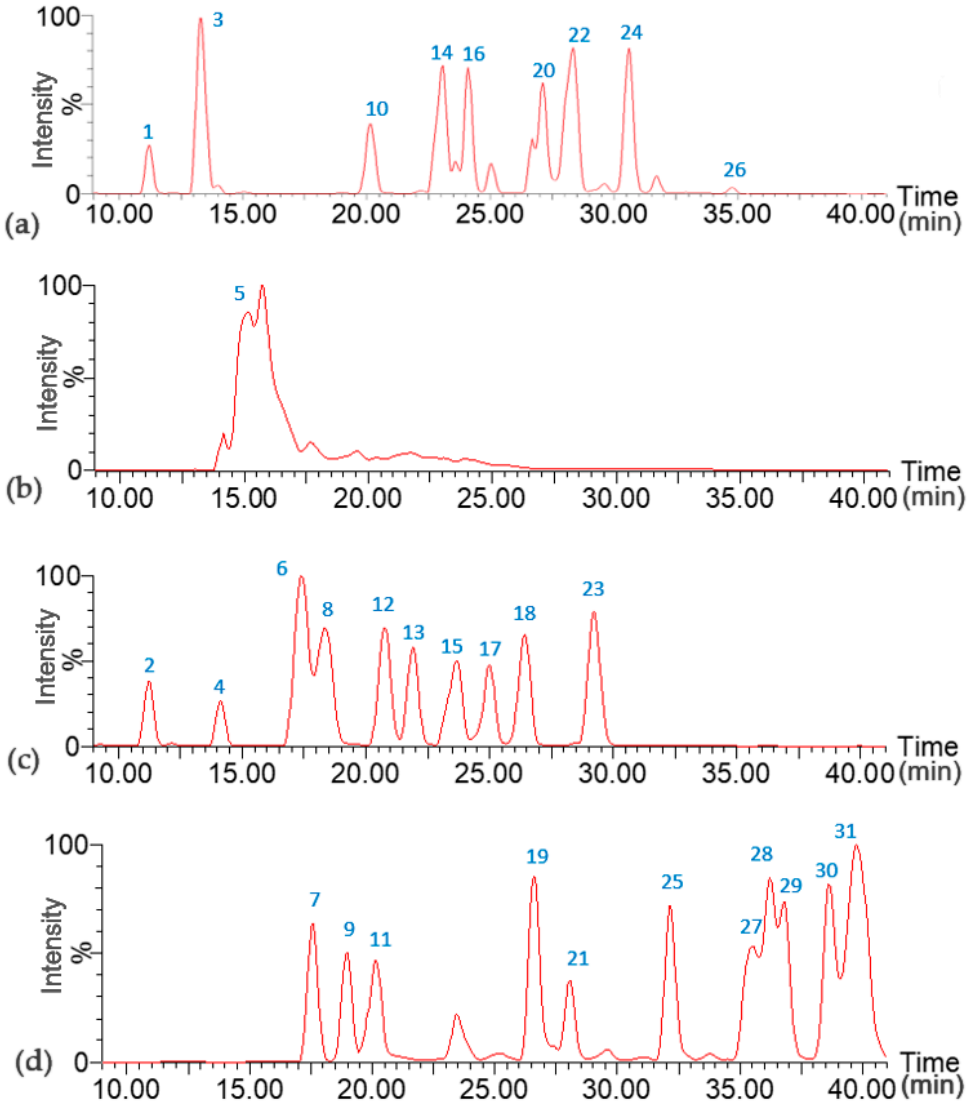

Figure 1. UPLC-ESI-QTOF-HRMS extracted ion chromatograms of piperamides from Piper nigrum cultivated in Costa Rica. $[M + H]^+$: (**a**) 274, 276, 330, 356, 358, 384, 398, 412, 426; (**b**) 286; (**c**) 272, 288, 314, 312, 340, 342, 344, 368, 370, 396; (**d**) 326, 328, 224, 386, 382, 332, 334, 332, 336, 346, 362. Peak numbers correspond to assignation as described in Table 1.

As stated, each chromatogram shows the corresponding extracted $[M + H]^+$ ion for the respective compounds listed in Table 1 and discussed in this section. The first group of piperamides has a characteristic methylenedioxyphenyl moiety and an isobutyl bonded to the amide group (Figure 2). These compounds were identified by the characteristic fragments of $[M + H - 73]^+$ due to the loss of the isobutylamine and $[M + H - 101]^+$ from the loss of the amide group along with the isobutyl chain. Both fragmentations could occur with an additional CH_2O loss from the methylenedioxy group cleavage, which generated the corresponding fragments at $[M + H - 103]^+$ and $[M + H - 131]^+$. An additional fragment at 135 Da was due to the rupture of the central chain to obtain a methylbenzodioxole group [20,21]. Finally, an ion at 161 Da was present because of the propenylbenzodioxole fragment [22].

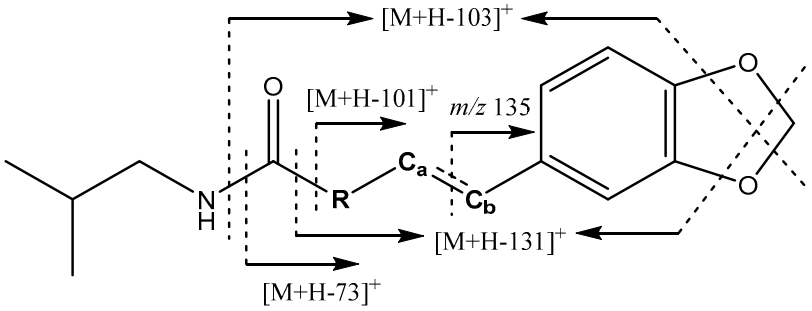

(**a**)

Compound	R	C_a-C_b
1	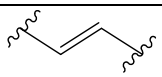	C=C
3	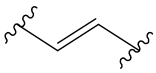	C-C
9	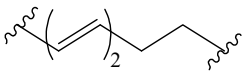	C=C
10	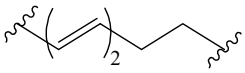	C-C
14	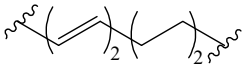	C=C
16	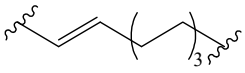	C=C
20	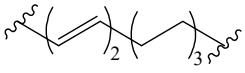	C=C
21	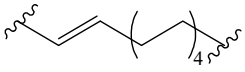	C=C
24	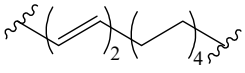	C=C
26	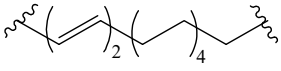	C=C

(**b**)

Figure 2. (**a**) Structure and main fragments for piperamides with a methylenedioxyphenyl moiety and an isobutyl amine substituent. (**b**) R chain and C_a-C_b bonding for each piperamide in this group.

For instance, peaks **1** and **3** (Figure 1a) correspond to piperloguminine and dihydropiperlonguminine, respectively. Peak **1** shows fragments at 201 Da $[M + H - 73]^+$, 173 Da $[M + H - 101]^+$, and 135 Da, while peak **3** has fragments at 173 Da $[M + H - 101]^+$, 145 Da $[M + H - 131]^{+,}$ and 135 Da. In turn, peak **9** (Figure 1a) corresponds to retrofractamide A, and peak **14** (Figure 1d) corresponds to retrofractamide B, both with fragments at $[M + H - 73]^+$, $[M + H - 101]^+$, 161 Da, and 135 Da. Peak **10** (Figure 1a) is identified as pipercallosine and shows fragments 135 Da and $[M + H - 101]^+$ at 229 Da, while peak **16** (Figure 1a) corresponds to piperchabamide D with fragments at 285 Da $[M + H - 73]^+$, 227 Da $[M + H - 131]^+$, and 135 Da.

In turn, peak **20** (Figure 1a), identified as guineensine, shows fragments $[M + H - 73]^+$ at 311 Da and $[M + H - 101]^+$ at 283 Da, plus the two fragments of benzodioxole moiety corresponding to 161 and 135 Da. In peak **21** (Figure 1d), corresponding to piperflaviflorine A, fragments are present at 313 Da $[M + H - 73]^+$ and 135 Da, while peak **24** (Figure 1a) corresponds to brachistamide B and exhibits fragments at 339 Da $[M + H - 73]^+$, 311 Da

$[M + H - 101]^+$, 161 Da, and 135 Da. The last compound in this group is peak **26** (Figure 1a), assigned to brachistamide D, with a characteristic main fragment at 135 Da [20,22–27].

When the side chain is a pyrrolidine ring instead of the isobutyl group (Figure 3), the fragments produced are $[M + H - 71]^+$ from the loss of this pirrolydine moiety and $[M + H - 99]^+$ from the loss of pyrrolidine along with the carbonyl group. Additional loss of CH_2O (30 Da) from the methylenedioxy group results, in these cases, in the loss of $[M + H - 101]^+$ and $[M + H - 129]^+$, respectively [20,21].

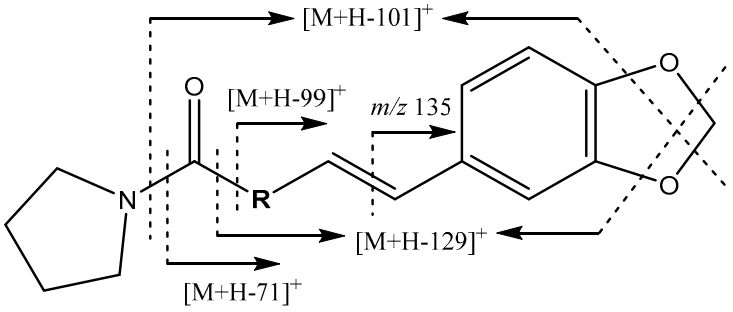

(**a**)

Compound	R
2	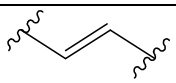
7	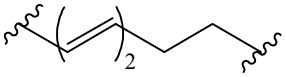
19	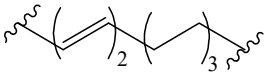

(**b**)

Figure 3. (**a**) Structure and main fragments for piperamides with a methylenedioxyphenyl moiety and a pyrrolidine cycle. (**b**) R chain for each piperamide in this group.

This pattern led to the identification of peak **2** (Figure 1c) as piperyline, showing fragments at $[M + H - 71]^+$ (201 Da), $[M + H - 101]^+$ (171 Da), $[M + H - 129]^+$ (143 Da), and 135 Da. In turn, peak **7** (Figure 1d) corresponds to (2*E*,4*E*,8*E*)-Piperamide-C9:3) and exhibits fragments at 227 Da $[M + H - 99]^+$ and 197 Da $[M + H - 129]^+$; peak **19** (Figure 1d), assigned to brachiamide A, presents fragments at 311 Da $[M + H - 71]^+$, 283 Da $[M + H - 99]^+$, 161 Da, and 135 Da [8,28,29].

The side chain can also be a piperidine ring. In this group of compounds, the loss of piperidine moeity gives the fragment at $[M + H - 85]^+$, while the loss of the amide produces the ion at $[M + H - 113]^+$. In both cases, an additional loss of CH_2O generates the fragments $[M + H - 115]^+$ and $[M + H - 143]^+$ (Figure 4) [20,21].

Peak **4** (Figure 1c) corresponds to piperanine and is identified by fragments at 203 Da $[M + H - 85]^+$, 175 Da $[M + H - 113]^+$, 145 Da $[M + H - 143]^+$, as well as 161 Da and 135 Da. Peak **5** (Figure 1b), identified as piperine, holds fragments at 201 Da $[M + H - 85]^+$, 171 Da $[M + H - 115]^+$, 143 Da $[M + H - 143]^+$, and 135 Da. In turn, peak **6** (Figure 1c), assigned to piperdardine, exhibits fragments at 199 Da $[M + H - 115]^+$ and 161 Da, while peak **8** (Figure 1c) corresponds to piperettine and has fragments at 227 Da $[M + H - 85]^+$, 199 Da $[M + H - 113]^+$, and 169 Da $[M + H - 143]^+$. Furthermore, peak **12** (Figure 1c), dehydropipernonaline, shows fragments $[M + H - 85]^+$ at 255 Da, $[M + H - 113]^+$ at 227 Da, 161 Da, and 135 Da and an additional fragment at 179 Da from the loss of the propenylbenzodioxole moiety [8,19,20,23,28,30,31].

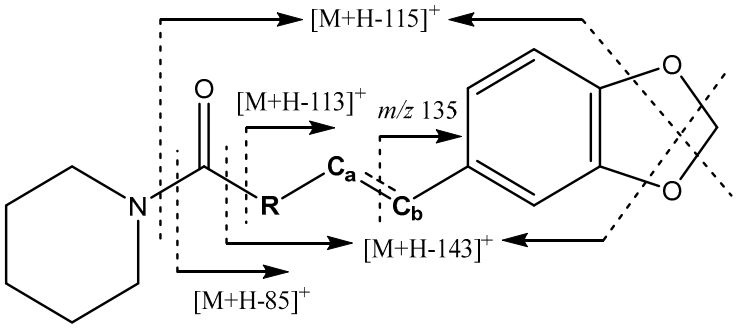

(**a**)

Compound	R	C_a-C_b
4	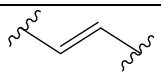	C-C
5	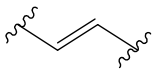	C=C
6	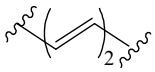	C-C
8	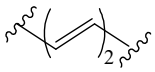	C=C
12	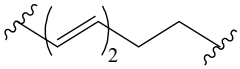	C=C
13	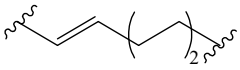	C=C
15	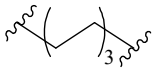	C=C
17	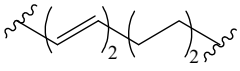	C=C
18	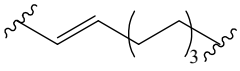	C=C
23	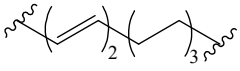	C=C

(**b**)

Figure 4. (**a**) Structure and main fragments for piperamides with a methylenedioxyphenyl moiety and a piperidine ring. (**b**) R chain and C_a-C_b bonding for each piperamide in this group.

Peak **13** (Figure 1c) corresponds to pipernonaline, with fragments at 229 Da [M + H − 113]$^+$, 227 Da [M + H − 115]$^+$, 199 Da [M + H − 143]$^+$, 161 Da, and 135 Da. The main fragments of peak **15** (Figure 1c), identified as piperolein B, are shown at 201 Da [M + H − 143]$^+$ and 135 Da, while peak **17** (Figure 1c), piperundecalidine, exhibits fragments at 255 Da [M + H − 113]$^+$ and 135 Da. Peak **18** (Figure 1c), assigned to piperchabamide B, has fragments at 285 Da [M + H − 85]$^+$, 161 Da, and 135 Da, while the last compound in this group, peak **23** (Figure 1c), corresponds to piperchabamide C and holds fragments at 311 Da [M + H − 85]$^+$, 283 Da [M + H − 113]$^+$, 161 Da, and 135 Da [8,19,20,23,28,30,31].

On the other hand, peak **22** (Figure 1a), identified as piperflaviflorine B, possesses a different fragmentation pattern (Figure 5), with fragments at 311 Da ([M + H − 87]$^+$) and 283 Da ([M + H − 115]$^+$), suggesting the presence of a 2-methylbutyl group in the amide, as previously described in the literature [32], and fragments at 161 Da and 135 Da are characteristic of the methylenedioxyphenyl moiety [32].

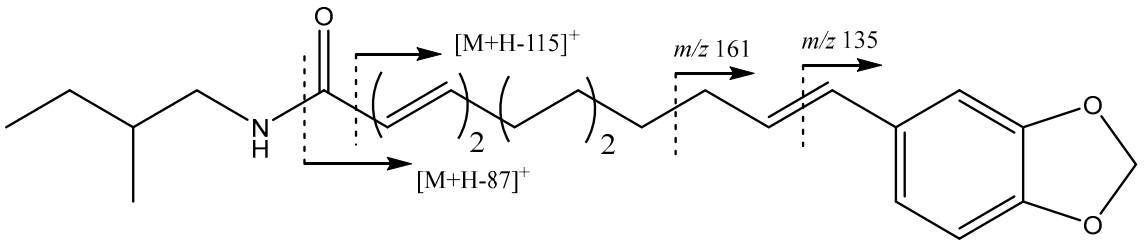

Figure 5. Structure and main fragments for piperflaviflorine B **22**.

The remaining group of peaks lacks the methylenedioxyphenyl group in their structures (Figure 6). Peak **11** (Figure 1d), assigned to pellitorine, shows fragments of an aliphatic unsaturated chain at 208 Da $[M + H - CH_4]^+$, 168 Da $[M + H - C_4H_8]^+$, and 154 Da $[M + H - C_5H_{10}]^+$ [29,33]. Peaks **25** and **28** (Figure 1d) were identified as isomers 1-(octadeca-2*E*,4*E*,12/13*Z*-trienoyl)pyrrolidine, with fragments at 261 Da $[M + H - 71]^+$ and 233 Da $[M + H - 99]^+$ from the loss of pyrrolidine and pyrrolidine amide, respectively, and an additional fragment at 304 Da $[M + H - C_2H_4]^+$ [28,34], not showing fragments at 135 Da or 161 Da or the additional loss of 30 Da of CH_2O from the methylenedioxyphenyl group.

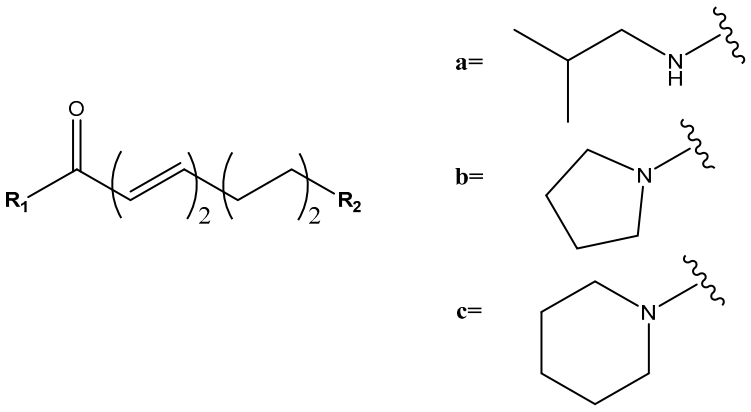

(**a**)

Compound	R_1	R_2
11	a	-CH_3
25	b	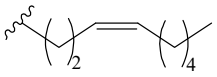
27	a	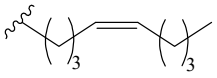
28	b	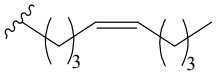
29	a	
30	c	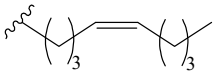
31	a	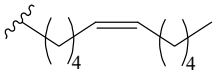

(**b**)

Figure 6. (**a**) Structure for piperamides with an aliphatic unsaturated olefinic chain. (**b**) R_1 and R_2 substituents for each piperamide in this group.

The fragment at $[M + H - 73]^+$ originated from the loss of isobutylamine, indicating the presence of an isobutyl lateral chain in peak **27** (Figure 1d) (2*E*,4*E*,13*Z*)-*N*-isobutyl-2,4,13-octadecatrienamide, peak **29** (Figure 1d) (2E,4E)-N-Isobutyl-2,4-octadecadienamide), and peak **31** (Figure 1d) (2*E*,4*E*,14*Z*)-*N*-Isobutyl-2,4,14-eicosatrienamide. Other observed fragments correspond to the rupture of the olefinic chain as $[M + H - CH_4]^+$ in peak **29**, $[M + H - C_2H_4]^+$ in peak **27**, and $[M + H - C_4H_8]^+$ in the three described peaks [28,35,36].

Finally, peak **30** (Figure 1d), assigned to 1-(octadeca-2E,4E,13Z-trienoyl)piperidine, had a fragment pertaining to the aliphatic unsaturated chain at $[M + H - C_2H_4]^+$ and another at $[M + H - 85]^+$ from the loss of piperidine [20,35].

3.2. Piperamides Quantification

The quantification of piperamides was carried out via UPLC-DAD with respect to a calibration curve of a piperine standard, with results expressed as mg of piperine equivalents (PE) per 100 g of dry sample and as a percentage of each piperamide in the extract composition, as described in the Materials and Methods section. Results are summarized in Table 2.

Table 2. Piperamides content in samples of *Piper nigrum* cultivated in Costa Rica.

Compound	Sample [1,2]		
	Pn-d	Pn-j	Pn-f
Piperylline	79.8 ^{h,i} ± 1.0 (1.6)	137.3 ^{e,f} ± 4.7 (1.6)	84 ^{g} ± 3.4 (1.4)
Piperlonguminine	48 ^{i} ± 0.6 (0.9)	80.8 ^{f} ± 3.8 (0.9)	70.4 ^{g} ± 4.4 (1.2)
Piperanine	n.q. [3]	116.2 ^{f} ± 2.9 (1.4)	72.6 ^{g} ± 1.8 (1.2)
Piperine [4]	2759 ^{a} ± 107 (54.0)	4514 ^{a} ± 94 (53.0)	2612 ^{a} ± 153 (44.0)
Pellitorine	414.4 ^{c} ± 5.2 (8.1)	725 ^{b} ± 35 (8.5)	570 ^{c} ± 38 (9.6)
Piperettine	178.1 ^{f,g} ± 1.9 (3.5)	185.9 ^{e} ± 5.9 (2.2)	119.6 ^{f,g} ± 2.1 (2.0)
(2*E*,4*E*,8*E*)-Piperamida-C9:3	105.7 ^{h,i} ± 1.3 (2.1)	141.5 ^{e,f} ± 4.4 (1.7)	121 ^{f,g} ± 10 (2.0)
Retrofractamide A	n.q.	84.8 ^{f} ± 6.3 (1.0)	82.9 ^{g} ± 2.7 (1.4)
Dehydropipernoline	123.3 ^{g,h} ± 1.1 (2.4)	201.5 ^{e} ± 5.7 (2.4)	165 ^{e,f,g} ± 7.0 (2.8)
Retrofractamide B	169 ^{f,g} ± 11 (3.3)	294.3 ^{d} ± 7.0 (3.5)	225 ^{e,f} ± 7.3 (3.8)
Piperolein B	n.q.	98.1 ^{f} ± 2.8 (1.2)	71.8 ^{g} ± 4.9 (1.2)
Guineensine	276.5 ^{d} ± 3.6 (5.4)	421 ^{c} ± 26 (4.9)	378.8 ^{d} ± 7.1 (6.4)
(2*E*,4*E*,13*Z*)-*N*-isobutyl-octadeca-2,4,13-trienamide	517.3 ^{b} ± 6.4 (10.1)	754 ^{b} ± 60 (8.9)	722 ^{b} ± 41 (12.2)
(2*E*,4*E*)-*N*-isobutyloctadecadienamide	189 ^{e,f} ± 14 (3.7)	315 ^{d} ± 11 (3.7)	264 ^{d,e} ± 23 (4.4)
1-(octadeca-2*E*,4*E*,12*Z*-trienoyl)piperidine	249.3 ^{d,e} ± 2.9 (4.9)	445 ^{c} ± 24 (5.2)	374 ^{d} ± 25 (6.3)

[1] Values are expressed in mg of piperine equivalent/100 g dry sample, and values in parentheses show the percent of total for each piperamide. [2] Different superscript letters in the row indicate differences are significant at $p < 0.05$ using one-way analysis of variance (ANOVA) with a Tukey post hoc as the statistical test. [3] n.q.: not quantifiable. [4] Piperine was quantified in a 1:5 dilution.

Regarding total piperamide contents, the Pn-j sample is the one with the highest value of 8514 mg PE/100 g dry material, which is 30% and 40% higher than the other two samples, Pn-f and Pn-d, respectively. This is in agreement with local producers' information that samples growing under less-rainfall conditions (Pn-j) are richer in contents than samples under higher-rainfall conditions (Pn-d and Pn-f). However, further studies would be needed, along with information on soil and other cultivation conditions, to evaluate their relationships with secondary metabolite content. With respect to the individual piperamides, piperine was the most abundant, which is in agreement with the literature [19,24,29], constituting between 44–54% of total piperamides, followed by (2*E*,4*E*,13*Z*)-*N*-isobutyl-octadeca-2,4,13-trienamide, ranging from 8.9 to 12.2%, and pellitorine, with values between 8.1 and 9.6%.

Compared with the literature, our values for piperine are within the range reported in previous studies, varying from 3320 to 5220 mg/100 g dry material [19,24,29]. With respect to the other piperamides, piperanine and piperlonguminine results are within the range that was reported in the literature, indicating values of 0.8–1.1% and 0.5–1.9% of total piperamides, respectively [19], while no quantification results were reported in the

literature for (2*E*,4*E*,13*Z*)-*N*-isobutyl-octadeca-2,4,13-trienamide, which is the piperamide with the second highest value in our study. In turn, results obtained for guineensine and pellitorine in Costa Rican black pepper dry fruits are higher than those reported by previous studies in the literature, which range between 0.76–1.18% and between 1.22–3.34%, respectively [24,29].

3.3. Semipreparative HPLC Analysis

Once piperine **5** was isolated from *P. nigrum* piperamides extracts through the procedure described in the Materials and Methods section, the remaining extract (SBN) was used for subsequent piperamides isolation through preparative and semipreparative HPLC separation. The solid isolated piperine **5** showed a molecular ion and fragmentation similar to the ones described in Section 3.1, and the HPLC-DAD analysis (Figure S1, Supplementary Materials) indicated 93% purity. ^{1}H and ^{13}C NMR analyses summarized in Figure S2 and Table S1 align with previous reports from the literature [28].

Main signals in the ^{1}H-NMR spectrum (Figure S2a) correspond to the three aromatic protons (δ 6.88–7.15 ppm) with the characteristic 1,3, 4-substitution coupling pattern and to four other protons in the olefinic region (δ 6.66–7.19 ppm), showing coupling constants (J = 14.5–15.6 Hz) consistent with *trans* alkene bonds. ^{13}C-NMR (Figure S2b) shows ten signals between δ 101.56 and 148.06 ppm corresponding to the aromatic and olefinic protons and a signal at low field (δ 165.01 ppm) that corresponds to the carbonyl group. An additional carbon is observed at δ 109.0 ppm that, along with the singlet at δ 5.90 ppm in the ^{1}H-NMR spectra, corresponds to the methylendioxy group. In the aliphatic region, there are no methyl groups, and two carbons at δ 40–50 ppm (^{13}C-NMR), along with the corresponding protons at δ 3.49 ppm (^{1}H-NMR), are explained by the bonding with the nitrogen in the piperidine ring.

HPLC preparative separation performed in the SBN remaining extract allowed us to isolate guineensine in fraction 8 and (2*E*,4*E*,12*Z*)-*N*-isobutyl-octadeca-2,4,12-trienamide in fraction 12, whose structures were confirmed by HRMS and NMR. In fact, fraction 8 showed a molecular ion and fragmentation consistent with guineensine **20** (Figure 7), as explained in Section 3.1. Figures S3 and S4 show the HPLC-DAD chromatogram and the ^{1}H and ^{13}C NMR spectra. Table S2 summarizes the shifts and coupling constants for these spectra.

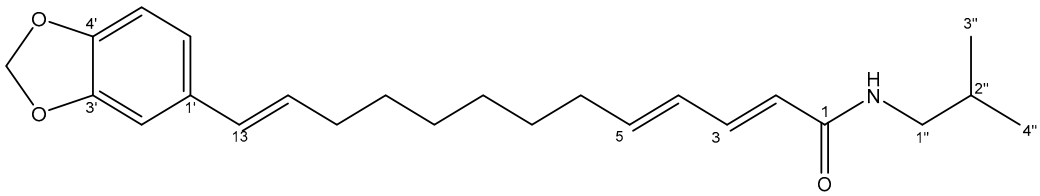

Figure 7. Structure of isolated guineensine **20**.

In fact, all signals shown in Table S2 and Figure S4 are coincident with the ones reported for guineensine in the literature [23]. For instance, the ^{13}C-NMR spectrum (Figure S4b) shows peaks at δ 166.7 ppm, corresponding to the carbonyl moiety, and at δ 100.9 ppm, characteristic of the methylenedioxy group, along with the singlet at δ 5.95 ppm in the ^{1}H-NMR spectrum (Figure S4a). In addition, the ^{13}C-NMR shows twelve signals in the unsaturated region, consistent with the aromatic ring (δ 105.4–147.9 ppm) that, along with the respective signals in the ^{1}H-NMR (δ 6.71–6.91 ppm), correspond to the coupling pattern for the 1,3,4 tri-substituted benzene ring.

The additional signals at δ 121.6, 128.3, 129.4, 141.5, and 143.3 ppm in the ^{13}C-NMR, along with the signals at δ 5.77, 5.99–6.15, 6.30, and 7.80 ppm in the ^{1}H-NMR, correspond to the olefinic signals with J = 15.0 and 15.8 Hz, indicating *trans* double bonds. Other representative signals are observed in the ^{13}C-NMR at δ 47.0 ppm that, along with the signal at δ 3.16 ppm (^{1}H-NMR), agree with C-N bonding and one important methyl signal

at δ 20.1 ppm that, along a doublet at δ 0.92 ppm (^{1}H-NMR), corresponds to an isobutyl group in the lateral chain of the amide.

Guineensine **20** was isolated with a yield of 209.7 mg/100 g dry black pepper, which is higher than reported in the literature. For instance, Nicolussi et al. [13] reported for *P. nigrum* an extraction with chloroform followed by column chromatography and preparative HPLC fractionation, obtaining 12.2 mg of purified guineensine (2.17 mg/100 g dry black pepper). On the other hand, Ramesh et al. [29] analyzed a methanolic extract of *P. nigrum* by HPTLC, obtaining 51 mg/100 g dry black pepper, while Rao et al. [24] obtained 48.9 mg/100 g dry black pepper for a methanolic extract analyzed by HPLC. Therefore, our results are higher than those in these reports, as well as the values obtained for guineensine isolated from *Piper longum* [13].

This result is important because of the different reported bioactive properties of guineensine, for instance, inhibiting endocannabinoid uptake [13] and significant neuropharmacological interactions when tested against CNS-related receptors, channels, and transporters [14]. In drug design studies for neuropathic pain regulation, bioactivity results obtained through quantitative structure–activity relationship (QSAR) model predictions found an association between bioactivity strength and chain length and molecular insights suggesting that the inhibitory mechanism may be related to the ability to initiate unstable vibrations in fatty acid hydrolase (FAAH)-like anandamide transporter [37]. Furthermore, guineensine's bioactivity goes beyond neuromodulation, having the ability to bind to and block the activities of two dual targets of secreted proteins and membrane-bound enzymes with high specificity from microbial pathogens [38].

Along with guineensine, (2*E*,4*E*,12*Z*)-*N*-isobutyl-octadeca-2,4,12-trienamide **25** was isolated in fraction 12 and characterized using HRMS and NMR. The molecular ion $[M + H]^+$ at 334 Da and fragmentation were consistent with the description (Section 3.1) for this trienamide **25** (Figure 8), which was obtained with a yield of 467.0 mg/100 g dry material. Figures S5 and S6 show the UPLC-DAD chromatogram and the ^{1}H and ^{13}C NMR spectra, and Table S3 summarizes the shifts and coupling constants for these spectra.

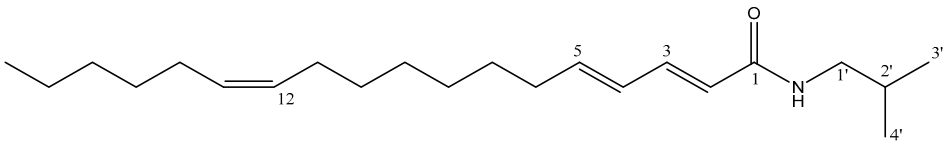

Figure 8. Structure of isolated (2*E*,4*E*,12*Z*)-*N*-isobutyl-octadeca-2,4,12-trienamide **25**.

The signals shown in Table S3 and Figure S6 for the ^{1}H and ^{13}C-NMR spectra are consistent with previous reports [23]. For instance, in the ^{13}C-NMR (Figure S6b), the carbonyl signal is observed at δ 166.4 ppm, and a total of six olefinic carbons are present (δ 121.7–143.3 ppm), while in the ^{1}H-NMR (Figure S6a), the signals between δ 5.36 and 7.21 ppm correspond to the six olefinic protons. Furthermore, the different coupling constants for four of them (J = 14.9–15.0 Hz) indicate their *trans* alkene bonding, while the other two olefinic protons (δ 5.36 ppm) have a low coupling constant, indicating a *cis* double bond. The isobutyl chain can be observed similarly as described for the previous compound, with a signal at δ 46.9 ppm (^{13}C-NMR) corresponding to the C-1′ bonded to the nitrogen, along with the signal at δ 3.18 ppm (^{1}H-NMR), and the two equivalent methyl groups at 20.1 ppm (^{13}C-NMR), along with a doublet signal at 0.91 ppm (^{1}H-NMR).

The isolation of this molecule is relevant because of previous reports on biological activities from similar compounds. For instance, (2*E*,4*E*,14*Z*)-*N*-isobutyleicosa-2,4,14-trienamide from *P. longum* exerted significant inhibitory effects on phenylephrine-induced mesenteric artery vasoconstriction [39], while another trienamide, 2*E*,4*E*,14*Z*)-*N*-(4-methylpentyl) octadeca-2,4,12-trienamide, identified in *P. nigrum*, exhibited important activity against larvae of *Aedes aegypti*, as determined by the World Health Organization (WHO) methodology [40]. In sensory studies, 1-(octadeca-2*E*,4*E*,13*Z*-trienyl)piperidine, among other similar compounds, displayed both a pungent impression and a long-lasting tingling sensation at

higher concentrations [28]. Furthermore, some dienamides and trienamides from the *Piper* genus have exhibited hepatoprotective activities on tumor necrosis factor (TNF-α)-induced cytotoxicity in L929 cells [41].

Fraction 4 from the aforementioned preparative HPLC consisted of a mixture of two main compounds; therefore, a semi-preparative HPLC separation was performed, as described in Section 2.7, resulting in the isolation of these two compounds, identified as pellitorine **11** and retrofractamide B **14** through HRMS and NMR analyses. In fact, the molecular ion $[M + H]^+$ at 224 Da and fragmentation were consistent with the description (Section 3.1) for pellitorine **11** (Figure 9), which was isolated with a yield of 361.8 mg/100 g dry material. Figures S7 and S8 show the UPLC-DAD chromatogram and the ^{1}H and ^{13}C NMR spectra.

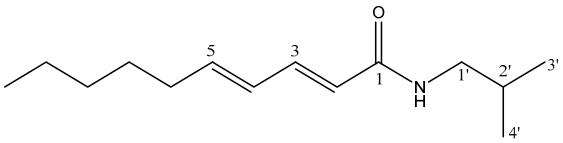

Figure 9. Structure of isolated pellitorine **11**.

^{1}H and ^{13}C NMR data shown in Table S3 and Figure S8 are consistent with literature [23]. For instance, ^{13}C-NMR (Figure S8b) shows a signal at δ 167.8 ppm consistent with the carbonyl group and four signals at δ 121.6–142.6 ppm from olefinic carbons with their corresponding protons at δ 5.77–7.21 ppm in the ^{1}H-NMR (Figure S8a) with coupling constants of J = 14.9–15.0 Hz, indicating *trans* alkene bonding. In addition, the signals at δ 46.6 and δ 19.1 ppm (^{13}C-NMR), along with the doublets at δ 3.08 and 0.94 ppm (^{1}H-NMR), are attributed to C-1′ and the two equivalent methyl groups, characteristic of the isobutyl moiety.

These results are relevant because of pellitorine's different reported bioactivities. For instance, its anti-inflammatory effects, along with piperine, were reported to inhibit the production of inflammatory factors and to reduce oxidative damage, attenuating the production of ROS [42]. In fact, in vitro and in mouse model studies proved promising for severe vascular inflammatory diseases, like sepsis and septic shock, because of pellitorine inhibiting the release of the high-mobility group box 1 (HMGB1) triggered by lipopolysaccharide and cecal ligation and puncture [43]. Previous pharmacokinetic tests found that pellitorine could cross the colorectal adenocarcinoma (Caco-2) cells monolayer and the rat gut when administered orally, and in the case of intravenous administration in mice, pellitorine also showed rapid penetration of the blood–brain barrier into the brain parenchyma, supporting the potential use of *Anacyclus pyrethrum* extract, containing pellitorine, in treating central nervous system diseases [44]. Furthermore, pellitorine has been found to display strong cytotoxicity against human leukemic cell line 60 (HL60) and Michigan Cancer Foundation-7 (MCF-7) cancer cells [45] as well as to exhibit anticoagulant effects in mice [46].

Finally, the molecular ion $[M + H]^+$ at 256 Da and fragmentation were consistent with the description (Section 3.1) for retrofractamide B **14** (Figure 10), which was obtained with a yield of 134.0 mg/100 g dry material. Figures S9 and S10 show the UPLC-DAD chromatogram and the ^{1}H and ^{13}C NMR spectra.

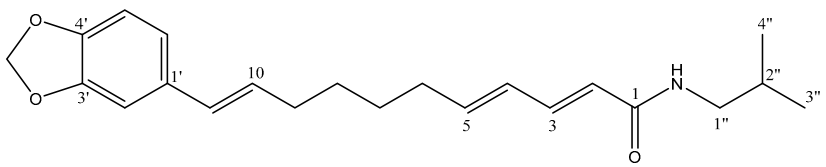

Figure 10. Structure of isolated retrofractamide B **14**.

The data in Table S2 and Figure S10 for the ^{1}H and ^{13}C-NMR spectra of retrofractamide B **14** are consistent with those in the previous literature [23]. The ^{13}C-NMR spectrum (Figure S10b) shows a signal at δ 167.8 ppm, corresponding to the carbonyl group, and another at δ 100.8 ppm, which is consistent with the methylenedioxy carbon. In addition, twelve signals in the double-bond region are observed (δ 100.8–148.0 ppm), which correspond to the 1,3,4 tri-substituted aromatic ring and the three double bonds. Finally, eight aliphatic carbons, including one signal at δ 46.6 ppm from C-1″ bonded to the nitrogen and two methyl groups at δ 19.1 ppm from the isobutyl moiety, are observed. With respect to ^{1}H-NMR signals (Figure S10a), the singlet at δ 5.92 ppm corresponds to the methylenedioxy protons, and signals at δ 6.73, 6.78, and 6.92 ppm pertain to the aromatic ring. In addition, the coupling constants for the olefinic protons (J = 15.1–15.8 Hz) indicate the *trans* double bonds. Finally, the doublets at δ 3.08 ppm and δ 0.94 ppm correspond to H-1″ and the two equivalent methyl groups from the isobutyl chain, respectively.

Several studies have reported different biological activities for retrofractamide B. For instance, some authors proposed that besides piperine, retrofractamide B can be responsible for the transient receptor potential vanilloid 1 (TRPV1) activation [47,48]. TRPV1 has become an attractive target for many pathologies, as its activation has roles in the pathogenesis of chronic inflammatory skin diseases, thermogenesis [48], diabetes, and bladder and lung function [49]. Retrofractamide B has been found to significantly increase the accumulation of triglyceride levels and to promote adipogenesis of 3T3-L1 cells [50]. In turn, *P. nigrum* extract containing retrofractamide Bm, along with piperine, pellitorine, and guineensine, has been reported to improve cell viability in neurotoxin 6-hydroxydopamine-induced SK-N-SH and SH-SY5Y (human neuroblastoma cell lines), showing the characteristics of amide alkaloids and their neuroprotective activities [51].

Compared with the literature, no previous isolation yield has been reported for the (2*E*,4*E*,12*Z*)-*N*-isobutyl-octadeca-2,4,12-trienamide, and in the case of pellitorine and retrofractamide B, our results yield higher values than those reported by previous studies on *Piper nigrum* from Korea [52,53] and India [54]. Therefore, these results, along with the high yields obtained for the (2*E*,4*E*,12*Z*)-*N*-isobutyl-octadeca-2,4,12-trienamide and guineensine, indicate the interest in further phytochemical and bioactivity studies of these Costa Rican species extracts and their isolated piperamides.

4. Conclusions

The analysis of piperamides-enriched extracts from *P. nigrum* commercial dry fruits cultivated in Costa Rica using the UPLC-QTOF-ESI MS technique allowed us to characterize a total of 31 different piperamides with and without a methylenedioxyphenyl moiety in their structures and with different *N*-substituents, including piperidine, pyrrolidine, isobutyl, and 2-methylbutyl groups. UPLC-DAD analyses enabled the quantification of 15 piperamides with values within the range reported in previous studies, such as the ones from piperine, piperyline, piperanine, and piperlonguminine, or higher than those from the literature, such as those obtained for guineensine and pellitorine. Furthermore, besides piperine, four other piperamides, namely retrofractamide B, pellitorine, (2*E*,4*E*,12*Z*)-*N*-isobutyl-octadeca-2,4,12-trienamide, and guineensine, were isolated with excellent yields, higher than literature findings. These results, along with the presence of diverse piperamides, which are reported for the first time for *P. nigrum* cultivated in Costa Rica, suggest the potential of these extracts for further research. Hence, structure–activity relationship studies can contribute to the increase in knowledge on fruits as a source of dietary compounds and their associated bioactivities with potential health benefits.

Supplementary Materials: The following supporting information can be downloaded at: https://www.mdpi.com/article/10.3390/horticulturae9121323/s1, Figure S1: HPLC-DAD chromatogram for isolated piperine **5**; Figure S2: (a) ^{1}H-RMN (b) ^{13}C-RMN from isolated piperine **5**; Table S1: ^{1}H and ^{13}C NMR shifts for isolated piperine **5**; Figure S3: HPLC-DAD chromatogram for isolated guineensine **20**; Figure S4: (a) ^{1}H-RMN (b) ^{13}C-RMN from isolated guineensine **20**. Table S2: Shifts for ^{1}H and ^{13}C NMR analysis of guineensine **20** and retrofractamide B **14**; Figure S5: UPLC-DAD chromatogram from

isolated (2*E*,4*E*,12*Z*)-*N*-isobutyl-octadeca-2,4,12-trienamide **25**; Figure S6: (a) ^{1}H-RMN (b) ^{13}C-RMN from isolated (2*E*,4*E*,12*Z*)-*N*-isobutyl-octadeca-2,4,12-trienamide **25**; Table S3: Shifts for ^{1}H and ^{13}C NMR analysis of pellitorine **11** and (2*E*,4*E*,12*Z*)-*N*-isobutyl-octadeca-2,4,12-trienamide **25**; Figure S7: UPLC-DAD chromatogram from isolated pellitorine **11**; Figure S8: (a) ^{1}H-RMN (b) ^{13}C-RMN from isolated pellitorine **11**; Figure S9: UPLC-DAD chromatogram from isolated retrofractamide B **14**; Figure S10: (a) ^{1}H-RMN (b) ^{13}C-RMN from isolated retrofractamide B **14**.

Author Contributions: Conceptualization, L.F.V.-H. and M.N.-H.; methodology, M.N.-H., A.M.A.-S. and L.F.V.-H.; formal analysis, L.F.V.-H., A.S.-K.; investigation, L.F.V.-H., M.N.-H., A.M.A.-S. and L.D.A.-C.; resources, M.N.-H., A.S.-K. and A.M.A.-S., data curation, L.F.V.-H., M.N.-H., A.M.A.-S. and A.S.-K.; writing—original draft preparation, L.F.V.-H., A.S.-K. and L.D.A.-C.; writing—review and editing, M.N.-H. and A.M.A.-S.; supervision, M.N.-H. and A.M.A.-S.; project administration, M.N.-H.; funding acquisition, M.N.-H. and A.M.A.-S. All authors have read and agreed to the published version of the manuscript.

Funding: This work was partially funded by grants from the University of Costa Rica (115-B6-163, 115-C0-001, 115-C3-005, ED-2033).

Data Availability Statement: The data from this study is in the manuscript and the corresponding supplementary material.

Acknowledgments: Authors thank the University of Costa Rica (UCR), the National Laboratory of Nanotechnology (LANOTEC) and the Costa Rica Institute of Technology (TEC).

Conflicts of Interest: The authors declare no conflict of interest.

References

1. Shan, B.; Cai, Y.Z.; Sun, M.; Corke, H. Antioxidant Capacity of 26 Spice Extracts and Characterization of Their Phenolic Constituents. *J. Agric. Food Chem.* **2005**, *53*, 7749–7759. [CrossRef] [PubMed]
2. Nair, K.P. *The Geography of Black Pepper (*Piper nigrum*): The "King" of Spices—Volume 1*; Springer International Publishing: Cham, Switzerland, 2020; ISBN 978-3-030-52864-5.
3. Srinivasan, K. Black Pepper (*Piper nigrum*) and Its Bioactive Compound, Piperine. In *Molecular Targets and Therapeutic Uses of Spices*; World Scientific: Singapore, 2009; pp. 25–64, ISBN 978-981-283-790-5.
4. Katarina, S.; Darinka, A.G.; Aleksandar, C.; Tatjana, R.; Bojana, V.; Mustafa, A. Piperine: Old Spice and New Nutraceutical? *Curr. Pharm. Des.* **2019**, *25*, 1729–1739. [CrossRef]
5. Wilhelm-Romero, K.; Quirós-Fallas, M.I.; Vega-Baudrit, J.R.; Guillén-Girón, T.; Vargas-Huertas, F.; Navarro-Hoyos, M.; Araya-Sibaja, A.M. Evaluation of Piperine as Natural Coformer for Eutectics Preparation of Drugs Used in the Treatment of Cardiovascular Diseases. *AAPS PharmSciTech* **2022**, *23*, 127. [CrossRef] [PubMed]
6. Takooree, H.; Aumeeruddy, M.Z.; Rengasamy, K.R.R.; Venugopala, K.N.; Jeewon, R.; Zengin, G.; Mahomoodally, M.F. A Systematic Review on Black Pepper *(Piper nigrum* L.): From Folk Uses to Pharmacological Applications. *Crit. Rev. Food Sci. Nutr.* **2019**, *59*, S210–S243. [CrossRef] [PubMed]
7. Yoon, M.; Jung, J.; Kim, M.; Lee, C.; Cho, S.; Um, M. Effect of Black Pepper (*Piper nigrum*) Extract on Caffeine-Induced Sleep Disruption and Excitation in Mice. *Nutrients* **2022**, *14*, 2249. [CrossRef] [PubMed]
8. Salehi, B.; Zakaria, Z.A.; Gyawali, R.; Ibrahim, S.A.; Rajkovic, J.; Shinwari, Z.K.; Khan, T.; Sharifi-Rad, J.; Ozleyen, A.; Turkdonmez, E.; et al. *Piper* Species: A Comprehensive Review on Their Phytochemistry, Biological Activities and Applications. *Molecules* **2019**, *24*, 1364. [CrossRef] [PubMed]
9. Onyesife, C.O.; Chukwuma, I.F.; Okagu, I.U.; Ndefo, J.C.; Amujiri, N.A.; Ogugua, V.N. Nephroprotective Effects of *Piper nigrum* Extracts against Monosodium Glutamate-Induced Renal Toxicity in Rats. *Sci. Afr.* **2023**, *19*, e01453. [CrossRef]
10. Lasso, P.; Rojas, L.; Arévalo, C.; Urueña, C.; Murillo, N.; Nossa, P.; Sandoval, T.; Chitiva, L.C.; Barreto, A.; Costa, G.M.; et al. *Piper nigrum* Extract Suppresses Tumor Growth and Enhances the Antitumor Immune Response in Murine Models of Breast Cancer and Melanoma. *Cancer Immunol. Immunother.* **2023**, *72*, 3279–3292. [CrossRef]
11. Turrini, E.; Sestili, P.; Fimognari, C. Overview of the Anticancer Potential of the "King of Spices" *Piper nigrum* and Its Main Constituent Piperine. *Toxins* **2020**, *12*, 747. [CrossRef]
12. Mitra, S.; Anand, U.; Jha, N.K.; Shekhawat, M.S.; Saha, S.C.; Nongdam, P.; Rengasamy, K.R.R.; Proćków, J.; Dey, A. Anticancer Applications and Pharmacological Properties of Piperidine and Piperine: A Comprehensive Review on Molecular Mechanisms and Therapeutic Perspectives. *Front. Pharmacol.* **2022**, *12*, 772418. [CrossRef]
13. Nicolussi, S.; Viveros-Paredes, J.M.; Gachet, M.S.; Rau, M.; Flores-Soto, M.E.; Blunder, M.; Gertsch, J. Guineensine is a novel inhibitor of endocannabinoid uptake showing cannabimimetic behavioral effects in BALB/c mice. *Pharmacol. Res.* **2014**, *80*, 52–65. [CrossRef] [PubMed]

14. Reynoso-Moreno, I.; Najar-Guerrero, I.; Escareño, N.; Flores-Soto, M.E.; Gertsch, J.; Viveros-Paredes, J.M. An Endocannabinoid Uptake Inhibitor from Black Pepper Exerts Pronounced Anti-Inflammatory Effects in Mice. *J. Agric. Food Chem.* **2017**, *65*, 9435–9442. [CrossRef] [PubMed]
15. Chatterjee, S.; Jain, S.; Jangid, R.; Sharma, M.K. Cytochrome P450 and P-Gp Mediated Herb–Drug Interactions of Some Common Indian Herbs. In *Studies in Natural Products Chemistry*; Elsevier: Amsterdam, The Netherlands, 2022; Volume 72, pp. 225–258, ISBN 978-0-12-823944-5.
16. Lieder, B.; Zaunschirm, M.; Holik, A.-K.; Ley, J.P.; Hans, J.; Krammer, G.E.; Somoza, V. The Alkamide Trans-Pellitorine Targets PPARγ via TRPV1 and TRPA1 to Reduce Lipid Accumulation in Developing 3T3-L1 Adipocytes. *Front. Pharmacol.* **2017**, *8*, 316. [CrossRef] [PubMed]
17. Lee, W.; Ku, S.-K.; Min, B.-W.; Lee, S.; Jee, J.-G.; Kim, J.A.; Bae, J.-S. Vascular Barrier Protective Effects of Pellitorine in LPS-Induced Inflammation In Vitro and In Vivo. *Fitoterapia* **2014**, *92*, 177–187. [CrossRef] [PubMed]
18. Morikawa, T.; Matsuda, H.; Yamaguchi, I.; Pongpiriyadacha, Y.; Yoshikawa, M. New Amides and Gastroprotective Constituents from the Fruit of *Piper chaba*. *Planta Med.* **2004**, *70*, 152–159. [CrossRef]
19. Friedman, M.; Levin, C.E.; Lee, S.U.; Lee, J.S.; Ohnisi-Kameyama, M.; Kozukue, N. Analysis by HPLC and LC/MS of pungent piperamides in commercial black, white, green, and red whole and ground peppercorns. *J. Agric. Food Chem.* **2008**, *56*, 3028–3036. [CrossRef]
20. Li, K.; Fan, Y.; Wang, H.; Fu, Q.; Jin, Y.; Liang, X. Qualitative and quantitative analysis of an alkaloid fraction from *Piper longum* L. using ultra-high performance liquid chromatography-diode array detector-electrospray ionization mass spectrometry. *J. Pharm. Biomed. Anal.* **2015**, *109*, 28–35. [CrossRef]
21. Chithra, S.; Jasim, B.; Anisha, C.; Mathew, J.; Radhakrishnan, E.K. LC-MS/MS Based Identification of Piperine Production by Endophytic *Mycosphaerella* sp. PF13 from *Piper nigrum*. *Appl. Biochem. Biotechnol.* **2014**, *173*, 30–35. [CrossRef]
22. Zaugg, J.; Baburin, I.; Strommer, B.; Kim, H.J.; Hering, S.; Hamburger, M. HPLC-based activity profiling: Discovery of piperine as a positive GABAA receptor modulator targeting a benzodiazepine-independent binding site. *J. Nat. Prod.* **2010**, *73*, 185–191. [CrossRef]
23. Li, K.; Zhu, W.; Fu, Q.; Ke, Y.; Jin, Y.; Liang, X. Purification of amide alkaloids from *Piper longum* L. using preparative two-dimensional normal-phase liquid chromatography reversed-phase liquid chromatography. *Analyst* **2013**, *138*, 3313–3320. [CrossRef]
24. Rao, V.R.S.; Raju, S.S.; Sarma, V.U.; Sabine, F.; Babu, K.H.; Babu, K.S.; Rao, J.M. Simultaneous determination of bioactive compounds in *Piper nigrum* L. and a species comparison study using HPLC-PDA. *Nat. Prod. Res.* **2011**, *25*, 1288–1294. [CrossRef] [PubMed]
25. Scott, I.M.; Jensen, H.R.; Philogène, B.J.R.; Arnason, J.T. A review of *Piper* spp. (Piperaceae) phytochemistry, insecticidal activity and mode of action. *Phytochem. Rev.* **2008**, *7*, 65–75. [CrossRef]
26. Banerji, A.; Sarkar, M.; Datta, R.; Sengupta, P.; Abraham, K. Amides from *Piper brachystachyum* and *Piper retrofractum*. *Phytochemistry* **2002**, *59*, 897–901. [CrossRef] [PubMed]
27. Okwute, S.K.; Egharevba, H.O. Piperine-Type Amides: Review of the Chemical and Biological Characteristics. *Int. J. Chem.* **2013**, *5*, 99–122. [CrossRef]
28. Dawid, C.; Henze, A.; Frank, O.; Glabasnia, A.; Rupp, M.; Büning, K.; Orlikowski, D.; Bader, M.; Hofmann, T. Structural and Sensory Characterization of Key Pungent and Tingling Compounds from Black Pepper (*Piper nigrum* L.). *J. Agric. Food Chem.* **2012**, *60*, 2884–2895. [CrossRef] [PubMed]
29. Ramesh, B.; Sarma, V.; Kumar, K.; Babu, K.S.; Devi, P.S. Simultaneous Determination of Six Marker Compounds in *Piper nigrum* L. and Species Comparison Study Using High-Performance Thin-Layer Chromatography–Mass Spectrometry. *J. Planar Chromatogr.* **2015**, *28*, 280–286. [CrossRef]
30. Liu, H.L.; Luo, R.; Chen, X.Q.; Ba, Y.Y.; Zheng, L.; Guo, W.W.; Wu, X. Identification and simultaneous quantification of five alkaloids in *Piper longum* L. by HPLC-ESI-MSn and UFLC-ESI-MS/MS and their application to *Piper nigrum* L. *Food Chem.* **2015**, *177*, 191–196. [CrossRef] [PubMed]
31. De Araujo, J.X.; Da-Cunha, E.V.L.; Maria, M.C.; Gray, A.I. Piperdardine, a piperidine alkaloid from *Piper tuberculatum*. *Phytochemistry* **1997**, *44*, 559–561. [CrossRef]
32. Shi, Y.N.; Liu, F.F.; Jacob, M.R.; Li, X.C.; Zhu, H.T.; Wang, D.; Cheng, R.R.; Yang, C.R.; Xu, M.; Zhang, Y.J. Antifungal Amide Alkaloids from the Aerial Parts of *Piper flaviflorum* and *Piper sarmentosum*. *Planta Med.* **2017**, *83*, 143–150. [CrossRef]
33. Scott, I.M.; Puniani, E.; Jensen, H.; Livesey, J.F.; Poveda, L.; Sánchez-Vindas, P.; Durst, T.; Arnason, J.T. Analysis of Piperaceae Germplasm by HPLC and LCMS: A Method for Isolating and Identifying Unsaturated Amides from *Piper* spp. Extracts. *J. Agric. Food Chem.* **2005**, *53*, 1907–1913. [CrossRef]
34. Da Luz, S.; Yamaguchi, L.; Kato, M.; De Lemos, O.; Xavier, L.; Maia, J.; Ramos, A.; Setzer, W.; Da Silva, J. Secondary Metabolic Profiles of Two Cultivars of *Piper nigrum* (Black Pepper) Resulting from Infection by *Fusarium solani* f. sp. Piperis. *Int. J. Mol. Sci.* **2017**, *18*, 2434. [CrossRef]
35. Kikuzaki, H.; Kawabata, M.; Ishida, E.; Akazawa, Y.; Takei, Y.; Nakatani, N. LC-MS Analysis and Structural Determination of New Amides from Javanese Long Pepper (*Piper retrofractum*). *Biosci. Biotechnol. Biochem.* **1993**, *57*, 1329–1333. [CrossRef]
36. Wei, K.; Li, W.; Koike, K.; Pei, Y.; Chen, Y.; Nikaido, T. New Amide Alkaloids from the Roots of *Piper nigrum*. *J. Nat. Prod.* **2004**, *67*, 1005–1009. [CrossRef] [PubMed]

37. Tou, W.I.; Chang, S.-S.; Lee, C.-C.; Chen, C.Y.-C. Drug Design for Neuropathic Pain Regulation from Traditional Chinese Medicine. *Sci. Rep.* **2013**, *3*, 844. [CrossRef]
38. Mgbeahuruike, E.E.; Yrjönen, T.; Vuorela, H.; Holm, Y. Bioactive Compounds from Medicinal Plants: Focus on *Piper* Species. *S. Afr. J. Bot.* **2017**, *112*, 54–69. [CrossRef]
39. Li, D.; Wang, R.; Cheng, X.; Yang, J.; Yang, Y.; Qu, H.; Li, S.; Lin, S.; Wei, D.; Bai, Y.; et al. Chemical Constituents from the Fruits of *Piper longum* L. and Their Vascular Relaxation Effect on Rat Mesenteric Arteries. *Nat. Prod. Res.* **2020**, *36*, 674–679. [CrossRef]
40. Siddiqui, B.S.; Gulzar, T.; Mahmood, A.; Begum, S.; Khan, B.; Afshan, F. New Insecticidal Amides from Petroleum Ether Extract of Dried *Piper nigrum* L. Whole Fruits. *Chem. Pharm. Bull.* **2004**, *52*, 1349–1352. [CrossRef]
41. Matsuda, H.; Ninomiya, K.; Morikawa, T.; Yasuda, D.; Yamaguchi, I.; Yoshikawa, M. Hepatoprotective Amide Constituents from the Fruit of *Piper chaba*: Structural Requirements, Mode of Action, and New Amides. *Bioorg. Med. Chem.* **2009**, *17*, 7313–7323. [CrossRef]
42. Duan, Z.; Xie, H.; Yu, S.; Wang, S.; Yang, H. Piperine Derived from *Piper nigrum* L. Inhibits LPS-Induced Inflammatory through the MAPK and NF-κB Signalling Pathways in RAW264.7 Cells. *Foods* **2022**, *11*, 2990. [CrossRef]
43. Ku, S.-K.; Lee, I.-C.; Kim, J.A.; Bae, J.-S. Anti-Septic Effects of Pellitorine in HMGB1-Induced Inflammatory Responses In Vitro and In Vivo. *Inflammation* **2014**, *37*, 338–348. [CrossRef]
44. Veryser, L.; Bracke, N.; Wynendaele, E.; Joshi, T.; Tatke, P.; Taevernier, L.; De Spiegeleer, B. Quantitative In Vitro and In Vivo Evaluation of Intestinal and Blood-Brain Barrier Transport Kinetics of the Plant *N*-Alkylamide Pellitorine. *Biomed Res. Int.* **2016**, *2016*, 5497402. [CrossRef] [PubMed]
45. Ee, G.C.L.; Lim, C.M.; Rahmani, M.; Shaari, K.; Bong, C.F.J. Pellitorine, a Potential Anti-Cancer Lead Compound against HL60 and MCT-7 Cell Lines and Microbial Transformation of Piperine from *Piper nigrum*. *Molecules* **2010**, *15*, 2398–2404. [CrossRef] [PubMed]
46. Ku, S.-K.; Lee, I.-C.; Kim, J.A.; Bae, J.-S. Antithrombotic Activities of Pellitorine In Vitro and In Vivo. *Fitoterapia* **2013**, *91*, 1–8. [CrossRef] [PubMed]
47. Panthong, S.; Imai, Y.; Matsuoka, T.; Suzuki, W.; Watanabe, T.; Terada, Y.; Kurohane, K.; Sekiguchi, K.; Ogawa, E.; Endo, Y.; et al. The Role of *Piper chaba* Hunt. and Its Pure Compound, Piperine, on TRPV1 Activation and Adjuvant Effect. *BMC Complement. Med. Ther.* **2020**, *20*, 134. [CrossRef] [PubMed]
48. Okumura, Y.; Narukawa, M.; Iwasaki, Y.; Ishikawa, A.; Matsuda, H.; Yoshikawa, M.; Watanabe, T. Activation of TRPV1 and TRPA1 by Black Pepper Components. *Biosci. Biotechnol. Biochem.* **2010**, *74*, 1068–1072. [CrossRef] [PubMed]
49. Brito, R.; Sheth, S.; Mukherjea, D.; Rybak, L.; Ramkumar, V. TRPV1: A Potential Drug Target for Treating Various Diseases. *Cells* **2014**, *3*, 517–545. [CrossRef] [PubMed]
50. Zhang, H.; Matsuda, H.; Nakamura, S.; Yoshikawa, M. Effects of Amide Constituents from Pepper on Adipogenesis in 3T3-L1 Cells. *Bioorganic Med. Chem. Lett.* **2008**, *18*, 3272–3277. [CrossRef]
51. Yu, L.; Hu, X.; Xu, R.; Ba, Y.; Chen, X.; Wang, X.; Cao, B.; Wu, X. Amide Alkaloids Characterization and Neuroprotective Properties of *Piper nigrum* L.: A Comparative Study with Fruits, Pericarp, Stalks and Leaves. *Food Chem.* **2022**, *368*, 130832. [CrossRef]
52. Park, I.-K.; Lee, S.-G.; Shin, S.-C.; Park, J.-D.; Ahn, Y.-J. Larvicidal Activity of Isobutylamides Identified in *Piper nigrum* Fruits against Three Mosquito Species. *J. Agric. Food Chem.* **2002**, *50*, 1866–1870. [CrossRef]
53. Ngo, Q.T.; Tran, P.T.; Tran, M.H.; Kim, J.A.; Rho, S.S.; Lim, C.-H.; Kim, J.-C.; Woo, M.H.; Choi, J.S.; Lee, J.-H.; et al. Alkaloids from *Piper nigrum* Exhibit Antiinflammatory Activity via Activating the Nrf2/HO1 Pathway: Alkaloids from *Piper nigrum* Activate the Nrf2/HO1 Pathway. *Phytother. Res.* **2017**, *31*, 663–670. [CrossRef]
54. Venkat Reddy, S.; Srinivas, P.V.; Praveen, B.; Hara Kishore, K.; China Raju, B.; Suryanarayana Murthy, U.; Madhusudana Rao, J. Antibacterial Constituents from the Berries of *Piper nigrum*. *Phytomedicine* **2004**, *11*, 697–700. [CrossRef] [PubMed]